Journal of Power Sources 195 (2010) 4990–4996

Contents lists available at ScienceDirect

Journal of Power Sources

journal homepage: www.elsevier.com/locate/jpowsour

On the room temperature synthesis of monoclinic Li_3FeF_6: A new cathode material for rechargeable lithium batteries

E. Gonzalo, A. Kuhn, F. García-Alvarado*

Universidad San Pablo-CEU, Departamento de Química, Urbanización Montepríncipe, Facultad de Farmacia, 28668 Boadilla del Monte, Madrid, Spain

ARTICLE INFO

Article history:
Received 10 November 2009
Received in revised form 24 January 2010
Accepted 13 February 2010
Available online 20 February 2010

Keywords:
Lithium batteries
Cathode materials
Intercalation reaction
Lithium iron fluoride
Electrochemical characterization
Ball milling

ABSTRACT

The α-polymorph of Li_3FeF_6 has been obtained at room temperature by a precipitation reaction from aqueous solution. This easy procedure that does not require any further annealing at high temperature yields a white powder with particles sizes ranging from 250 to 400 nm. After proper processing by mechanical milling, particle sizes clearly below 100 nm are achieved and this fluoride reacts reversibly with lithium at an average voltage of 3.1 V, which is expected for the Fe^{3+}/Fe^{2+} redox couple. After 12 h of ball milling observed average particle size is ca. 50 nm and a reversible capacity of 100 mA h g^{-1} is obtained. This corresponds to 70% of the theoretical capacity expected for the one electron reduction of Fe^{3+}. The mentioned capacity is fairly kept upon cycling making the new material useful as the positive electrode in lithium batteries. This is the very first time that a material for cathode application in lithium batteries is prepared at room temperature and from aqueous solution, a procedure which is easily scalable and hence of high industrial interest.

1. Introduction

The search for materials that may be useful as the cathode of rechargeable lithium batteries have produced a large number of candidates, see for example Refs. [1–13]. The variety of manifold materials is reduced mainly to two widely commercialized cathodes [1,4] once technological requirements, price, safety and toxicity are considered all together. The change from the expensive $LiCoO_2$ to the safer and cheaper $LiFePO_4$ produced myriads of works devoted to iron based electrodes. Most of them are related to the poly-oxoanionic compounds (such as $LiFePO_4$), but a few others have been investigated trying new approaches, as for example some reports on FeF_3 [14,15].

Fluorides are an interesting alternative as the high ionicity of the M-F bond produces a high redox potential [16] of the respective transition metal and, consequently, high operating voltage and high specific energy have been observed for several metal trifluorides [15]. Therefore, some attention has been also paid to the development of transition metal fluorides. Recently, ternary fluorides have been investigated as cathodes for sodium batteries because of the larger abundance, better distribution and low toxic nature of sodium when compared to lithium [17,18].

Although the high ionic nature of the M–F bond is advantageous to produce high energy cathode materials, it is at the same time responsible for the insulating behaviour exhibited by most fluorides. Therefore, similarly to $LiFePO_4$, fluorides suffer from poor electronic conductivity and slow kinetics of intercalation which limits the electrochemical performances of cells under a constant current. Ways to overcome the limitations encountered for $LiFePO_4$ have now been applied with success to fluorides as reported by several authors [14,17–19]. Therefore, it is obvious that fluorides may be extremely interesting candidates to cathodes in as much as some of them release output voltages in the same range as $LiFePO_4$ does. However, the main drawback of fluorides is the difficulty of the preparation (see Gocheva et al. [17] and references therein). On the other hand, high reactivity of fluorides is also a disadvantage. They tend to be unstable under humid atmosphere or water producing fluoride ions by hydrolysis reactions. This is the reason why mechanical milling has to be made under an inert atmosphere as described in the more recent works that have reported fluorides as possible cathode materials [14,17,18].

In this paper we report the competitive synthesis of a ternary fluoride with composition Li_3FeF_6, specifically its monoclinic (alpha) polymorph, which does not present the aforementioned limitations. It is prepared at room temperature; it does not produce hydrolysis, in fact it is slightly soluble in water. Furthermore, since it intercalates lithium reversibly at high voltage, this material is then an optimum candidate to new cathode materials for the next generation of lithium batteries [20].

Li_3FeF_6 has been known for a long time [21–23]. There are actually two known polymorphs of Li_3FeF_6, which are prepared by solid state reaction of LiF and FeF_3 under inert atmosphere using sealed

* Corresponding author. Tel.: +34 91 3724728; fax: +34 91 3510475.
E-mail address: flaga@ceu.es (F. García-Alvarado).

0378-7753/$ – see front matter © 2010 Elsevier B.V. All rights reserved.
doi:10.1016/j.jpowsour.2010.02.040

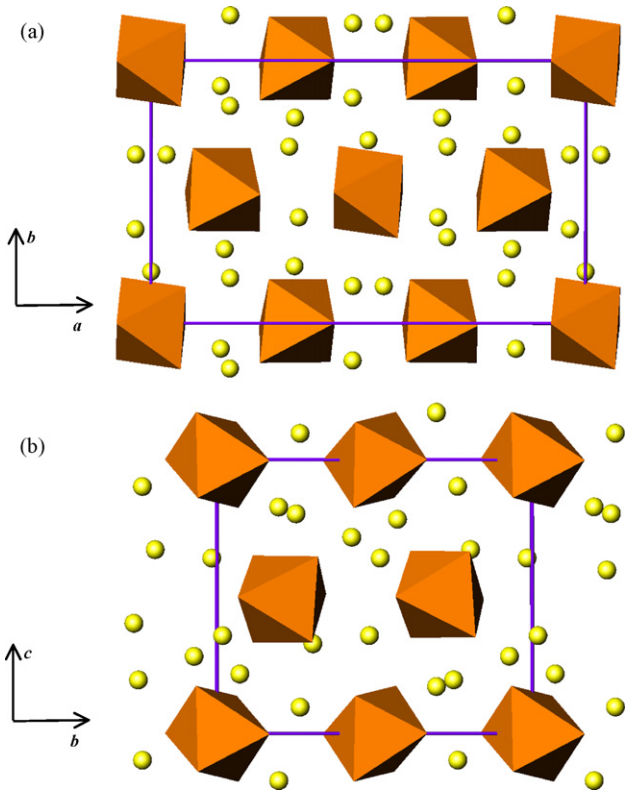

Fig. 1. View of the α-Li_3FeF_6 structure projected onto the *a*–*b* plane (a) and the *b*–*c* plane (b). It consists of isolated FeF_6 octahedra with interstitial Li atoms (spheres) which are 4-, 5- and 6-coordinated by F atoms.

gold or platinum ampoules. Tressaud et al. [22] prepared a monoclinic low temperature form (α-polymorph) at 300 °C, though the diffraction pattern could not be indexed. However, above 500 °C it transforms to an orthorhombic phase (β-polymorph) that was isolated by quenching and characterized by X-ray diffraction. Later on, Massa and Rüdorff [23] characterized not only the high temperature polymorph (β) but also the low temperature polymorph (α). There is a controversy in the denomination of both polymorphs. Monoclinic Li_3FeF_6 was reported [23] to be isostructural with β-Li_3AlF_6 [24–26], whereas orthorhombic Li_3FeF_6 was found to be isostructural with α-Li_3AlF_6 [27]. Consequently, some authors have chosen the designation of the monoclinic as the β and the orthorhombic as the α-form [23] contrarily to Tressaud et al. [22]. In this work the naming given by Tressaud et al. [22] will be used and hence the monoclinic polymorph of Li_3FeF_6 will be referred as α-Li_3FeF_6. However, we will also refer to it attending to its cell symmetry to avoid misunderstandings.

Both polymorphs are closely related to cryolite, and their crystal structures have been recently revisited by means of combined X-ray and neutron diffraction and electron microscopy [28]. Both structures consist of isolated and slightly distorted FeF_6 octahedra. The monoclinic polymorph is simply related to the orthorhombic polymorph by considering a tilt rotation of Fe–F_6 octahedra. These Fe–F_6 octahedra are linked together by a set of interconnected lithium polyhedra in the tri-dimensional structure (see Fig. 1). In cryolite, Na_3AlF_6, two different Na sites are found where Na is 6- and 8-coordinated by fluorine atoms. For Li_3FeF_6, however, 3 different Li environments are found in the orthorhombic phase, while 5 different Li polyhedra are present in the monoclinic phase. Four-, five- and six-coordinated Li atoms by fluorine atoms are found in both forms [28]. The structure of Li_3FeF_6 has the adequate topology to intercalate lithium, though never before a paper has been devoted to the intercalation chemistry of these fluorides. We report here for the first time the electrochemical properties of the monoclinic α-form of Li_3FeF_6. On the other hand, the corresponding electrochemical properties of the high temperature polymorph, β-Li_3FeF_6 are reported elsewhere [29].

2. Experimental

2.1. Preparation

Due to the difficult synthesis reported to obtain pure α-Li_3FeF_6 by the ceramic route [22] we have chosen an alternative aqueous solution-chemistry approach with precipitation of the ternary fluoride. Through this route the use of FeF_3, which is hygroscopic, is avoided.

Monoclinic α-Li_3FeF_6 has been prepared accordingly to the following chemical reaction [20]:

$$Fe(NO_3)_3{\cdot}9H_2O + 6HF + (3/2)Li_2CO_3 \rightarrow Li_3FeF_6 + (21/2)H_2O + (3/2)CO_2 + 3HNO_3$$

In a typical procedure the stoichiometric quantity of HF in aqueous solution (for example 40%) was added to a saturated aqueous solution containing the stoichiometric quantity of $Fe(NO_3)_3{\cdot}9H_2O$. Afterwards, the stoichiometric amount of Li_2CO_3 was added. The final solution was stirred for a few hours. After evaporation of solvent excess either at room temperature or by concentrating at mild temperature (50–60 °C) on a water bath, the obtained white powder is centrifuged and washed with small portions of water several times. Finally, the powder was dried either by washing with ethanol or by heating it at 80 °C for 1 h in a drying oven. The as-prepared powder is probably identical with that obtained by Nielsen in the 1930s [21], though no further structural data was given in that work to compare both products.

2.2. Structural and chemical characterization

Reaction products were analyzed by powder X-ray diffraction (XRD) on a Philips X'PERT-PRO diffractometer, operated at 50 kV and 45 mA, using monochromatic Mo $K\alpha_1\alpha_2$ ($\lambda = 0.71073$ Å) radiation obtained with a graphite monochromator and a PW1964 scintillation point detector. Selected angular range was $2\theta = 4°$–$50°$ with a 0.04°/10 s scan rate operated in continuous scan mode. Diffraction patterns were analyzed by the Rietveld method [30] using the FullProf program [31].

In addition, crystal symmetry was checked by means of Selected Area Electron Diffraction using a JEOL 2000FX electron microscope. The same apparatus was used to study the morphology and particle size of the as-prepared fluoride and the ball-milled samples (see below).

Chemical microanalysis was accomplished with X-ray energy dispersive spectroscopy (X-EDS) using the same microscope, which is equipped with an OXFORD INCA EDS detector. Numerous spectra were recorded and chemical Fe:F ratios were determined in order to analyse the homogeneity of the samples and the eventual presence of different types of particles. As lithium is not detectable by EDS, it was quantified by means of flame atomic absorption spectrometry using a Flame Sherwood 410 Photometer. For this purpose a given amount of sample (typically 50 mg) was leached in 2 mol L^{-1} hydrochloric acid.

Thermal stability has been analysed by TGA/DTA experiments using a Netzsch STA 409 apparatus. Samples were heated at 10 K min^{-1} up to 600 °C under commercial nitrogen. On the other hand, ex situ experiments were carried out by heating the sample at 500 and 600 °C under air. For both cases XRD patterns were recorded after thermal treatment.

2.3. Mechanical milling

The as obtained products and conductive carbon were ground by using a planetary-type ball mill Pulverisette 7 (Fritsch GmbH, Germany) in order to obtain a carbon-metal fluoride nanocomposite (CMFNC). The following conditions were used: sample weight 1 g; grinding media: 2 balls with a diameter of 10 mm; milling media and chamber material: zirconium dioxide; volume of grinding chamber: 20 mL; mill speed: 500 rpm, for different dry milling times ranging from 1 to 24 h in air.

2.4. Electrochemical characterization

The electrochemical behavior of Li_3FeF_6 was analyzed in non-aqueous CR2032-type coin cells. Each cell was assembled in an argon-filled glove box using a glass fibre separator (Aldrich) soaked with 1 M $LiPF_6$ in 1:1 (v/v) EC/DMC electrolyte. (EC = ethylenecarbonate, DMC = dimethylcarbonate). A 5 mm diameter lithium disk served as the negative electrode. The positive electrodes with loadings of approximately 30 mg were composed of 72% active material (Li_3FeF_6), 25% conducting carbon black and 3% PTFE (Aldrich) as binder, which were pressed into 8 mm diameter pellets. Galvanostatic lithium insertion/de-insertion reactions were performed with a MacPile II system (Biologic) at a constant current density of 0.1 mA cm^{-2} at 25 °C unless noted otherwise. Cells were typically cycled from the rest potential to 2 and 4.5 V, respectively.

3. Results and discussion

The precipitation method described in Section 2 produced a white powder. The corresponding X-ray diffraction pattern (see Fig. 2) can be fully indexed by using the space group and monoclinic cell symmetry given for β-Li_3AlF_6 [26]. A schematic representation of this structural type can be seen in Fig. 1 and in the inset of Fig. 2. Therefore, the obtained product corresponds to the monoclinic form of Li_3FeF_6 reported by Massa and Rüdorff [23], though these authors obtained it by high temperature reaction of the binary fluorides. We will also refer to the obtained fluoride as the α-polymorph. Refined lattice parameters of α-Li_3FeF_6 are: $a = 14.414(1)$ Å; $b = 8.6685(7)$ Å; $c = 10.0359(8)$ Å; $\beta_{mono} = 95.730(4)^\circ$. Space group is $C2/C$ (no. 15). A more detailed structural study of monoclinic (α) and orthorhombic (β) polymorphs of Li_3FeF_6 using combined X-ray and neutron diffraction will be published elsewhere [28]. The graphical result of the Rietveld refinement of α-Li_3FeF_6 is depicted in Fig. 2, where the difference between experimental and calculated diffraction patterns and the significant *R*-values are given.

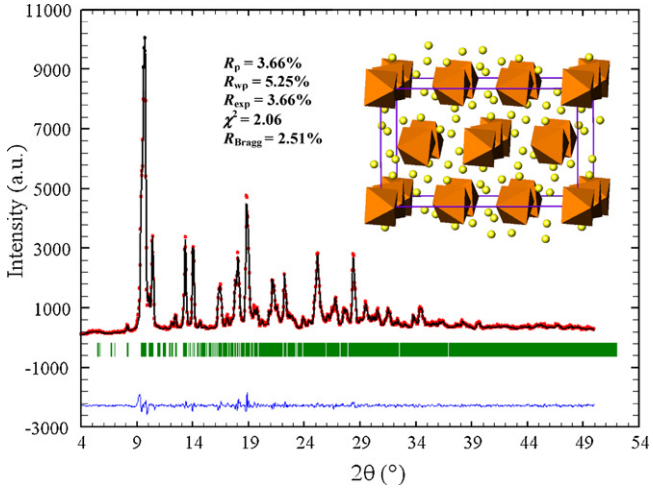

Fig. 2. Graphical result of the Rietveld refinement and reliability factors of fitting. [Fe–F_6] octahedral and Li (spheres) arrangements are shown in the inset.

The collection of electron diffraction patterns has been complicated by a generalized instability of α-Li_3FeF_6 under the highly energized electron beam probing the sample. This returned a progressive fast degradation of the specimens and the disappearance of diffraction spots in electron diffraction patterns with concentric blur due to the formation of amorphous regions. However, SAED patterns recorded showed the lattice spots of a C-centred monoclinic cell and can be fully indexed using a cell with $a \approx 14.4$ Å, $b \approx 8.7$ Å, $c \approx 10.0$ Å, $\beta_{mono} \approx 96^\circ$ characteristic of α-Li_3FeF_6 (see Fig. 3).

Fig. 4 shows a low magnification image of typical crystals viewed by Transmission Electron Microscopy (Fig. 4a), where its morphology and sizes are observed, together with a more general morphological observation and size distribution obtained by Scanning Electron Microscopy of the as-prepared material (Fig. 4b). The microscopy study reveals that α-Li_3FeF_6 obtained by the precipitation method produces submicrometric prismatic particles with an average particle size of 300 nm but highly distributed (250–400 nm in width).

EDS measurements have been performed in a large number of thin crystals in order to examine composition of powdered Li_3FeF_6 obtained by the precipitation method (see Fig. 5). We found that average percentages regarding Fe and F were homogenous and close to the nominal ratios (observed—Fe: 83%; F: 17%. Calculated–Fe: 85.7%; F 14.3%). Chemical analysis of lithium by flame atomic absorption spectrometry yielded that lithium content is 9.3% by weight, which is close to the expected content of Li for Li_3FeF_6 (10.9%).

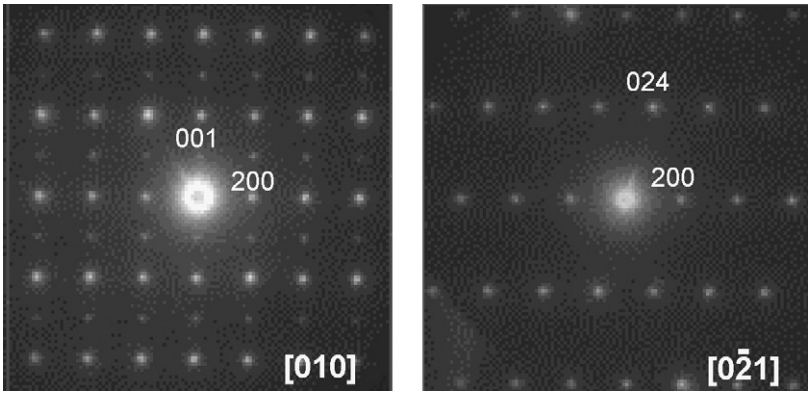

Fig. 3. Some SAED patterns of α-Li_3FeF_6 obtained along different zone axis.

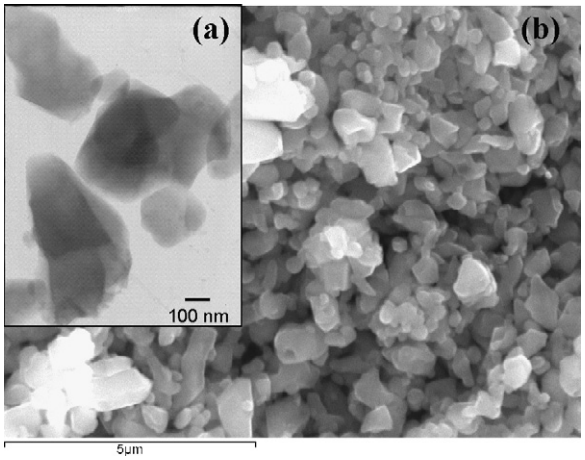

Fig. 4. Low magnification TEM (a) and SEM (b) images showing the typical shapes and sizes of α-Li_3FeF_6 crystals prepared by precipitation from aqueous solution.

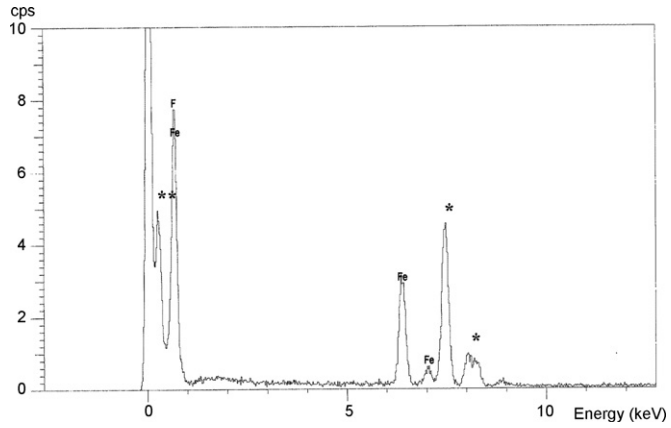

Fig. 5. Typical EDS spectrum showing the microanalysis performed on a α-Li_3FeF_6 sample obtained by the precipitation method. Peaks marked with asterisks come from the Ni grid (*) having a holey-carbon (**) film, on which the powdery fluoride sample was deposited.

The electrochemical behavior of a non-milled α-Li_3FeF_6 sample, which was manually mixed with carbon black and binder using a pestle and a mortar, is presented in Fig. 6. A low discharge capacity is developed when discharging to ca. 2.2 V. In any case the capacity involved is very small and cycling in that voltage region was rather poor (see inset of Fig. 6). Deep-discharging of cells produces a non-reversible pseudo-plateau located at ca. 1.2 V. X-rays taken from the cathode pellet at the end of the deep-discharge showed a high degree of amorphization of the final product, in which characteristic peaks of LiF besides broad peaks corresponding to α-Li_3FeF_6 are observed. This is a clear indication for a partial decomposition of α-Li_3FeF_6 at low voltage accordingly to the following reaction:

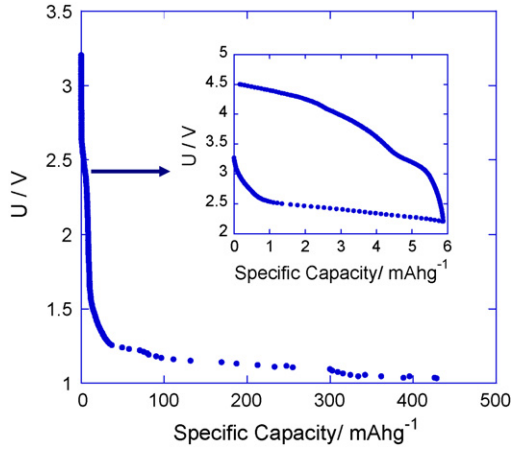

Fig. 6. First discharge down to 1 V of a cell using as-prepared α-Li_3FeF_6 as active material of the positive electrode (current density: 0.1 mA cm^{-2}). The inset shows the first discharge-charge cycle of a cell in a higher voltage range (2.2–4.5 V) for which a very low reversible capacity is observed.

$$Li_3FeF_6 + 3Li \rightarrow 6LiF + Fe \quad (1)$$

In the case of $LiFePO_4$ and other poor electronic conductors, intercalation is inhibited and only by proper processing high performances can be achieved [32–37]. The positive effect that has a proper processing, e.g. mechanical milling, could be demonstrated for other related insulating electrodes as for example the fluorides reported in ref. [14,17]. It is noteworthy to recall that not only improving of electronic conductivity by carbon coating is needed, because at the same time the diffusion path for lithium migration needs to be shortened in order to reach a high capacity at higher current rates. Therefore, particle size has to be reduced down to the nanoscale. The precipitation procedure followed to obtain α-Li_3FeF_6 does already provide submicrometric particle size in the range 250–400 nm (see Fig. 4). Particles are much smaller than those obtained for β-Li_3FeF_6 [29] which is prepared at high temperature. Badway's work on CMFNCs [14] showed that specific capacity of FeF_3 increased systematically with milling time due to reduction of particle size. Reduction of particle size below 40 nm allowed for the development of the highest capacity in FeF_3, reaching the theoretical capacity due to full reduction of Fe^{3+} to Fe^{2+}. Therefore, we have applied the same approach to the monoclinic polymorph (α) of Li_3FeF_6. Carbon coating and reduction of particle size has been carried out by dry ball milling the fluoride with carbon in air as described in Section 2.

As an example Fig. 7 shows typical low magnification TEM images of particle sizes obtained after 0 and 5 h of ball milling. It can be seen that particle sizes have been effectively decreased. Though still sizes are inhomogeneously distributed, the average particle size has been determined to be reduced from 300 nm to 100 and 50 nm after 5 and 12 h of ball milling, respectively. For 24 h particle size does not effectively decrease below 50 nm. EDS microanalysis performed at the different milling stages revealed that the Fe:F ratio remained at the typical values observed in the non-milled sample, indicating that the chemical composition of the fluoride was not affected by the mechanical milling procedure. On the other hand, XRD confirmed that structural integrity is also kept, though the reduction of particle size goes along with a decrease in the crystalline domain. As a consequence broadening of reflections was observed.

The positive effect that the decreasing of particle size has on the electrochemical behavior can be seen in Fig. 8. We only present the high voltage region (from 3.5 to 2.25 V on reduction and up to 4.5 V on oxidation) in as much as the long plateau observed at lower voltage (see Fig. 6) produced the decomposition of the fluoride. It can be seen that the number of lithium ions that react with the fluoride increases as a function of milling time (0–12 h) of the Li_3FeF_6/C nanocomposite. After the first cycle, electrodes were analyzed by XRD showing that the structure of monoclinic Li_3FeF_6 is kept, indicating that an intercalation reaction is taking place.

Simple manual mixing produced a poor electrochemical performance, whereas specific capacity increases with mechanical milling. The quantity of reversibly inserted lithium (per formula unit Li_3FeF_6) increases from 0.45 to 0.7 after milling times of 5 and 12 h, respectively, whereas milling during 24 h did not further improve capacity. This finding is in agreement with the fact that average particle size is reduced to ca. 50 nm after 12 h of milling; however no further remarkable decrease in particle size can be

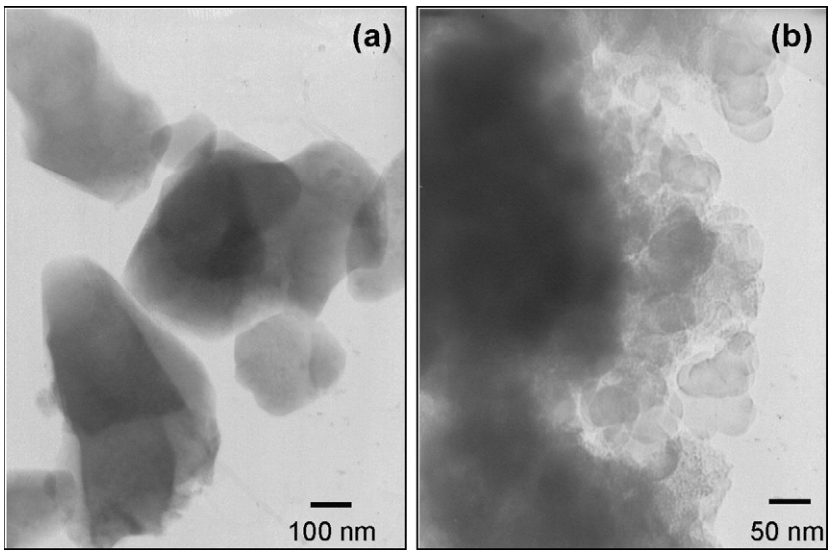

Fig. 7. Low magnification TEM images showing the differences in shapes and sizes of α-Li_3FeF_6 crystals after processing by ball milling with conductive carbon for (a) 0 h and (b) 5 h.

achieved for more than 12 h as it can be seen in the graph of Fig. 9 where variation of both particle size and capacity with milling time is depicted. On the other hand, Fig. 10 shows the good cycling behaviour of the composite obtained after 12 h of ball milling as an example.

Capacities at 0.1 mA cm^{-2} range from 65 to 100 mA h g^{-1} and correspond to 5 and 12 h of milling, respectively (see Fig. 9). The highest capacity achieved corresponds to 70% of theoretical capacity expected for the reduction of one Fe^{3+} to Fe^{2+} (140 mA h g^{-1}). That theoretical capacity may be achieved by further decreasing the particle size. However, we have not succeeded in reducing the particle size below 50 nm using our present experimental ball mill equipment.

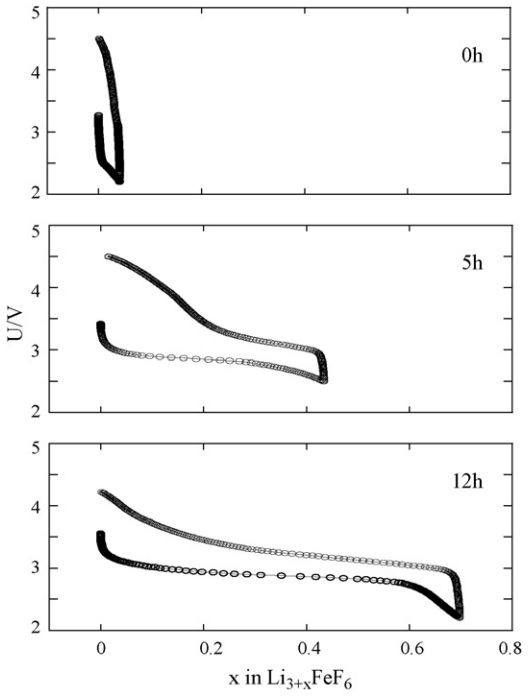

Fig. 8. First discharge-charge cycle of cells using conductive carbon + α-Li_3FeF_6 composites obtained by ball milling as the positive electrode. The different ball milling times used are indicated on the graphs (current density: 0.1 mA cm^{-2}).

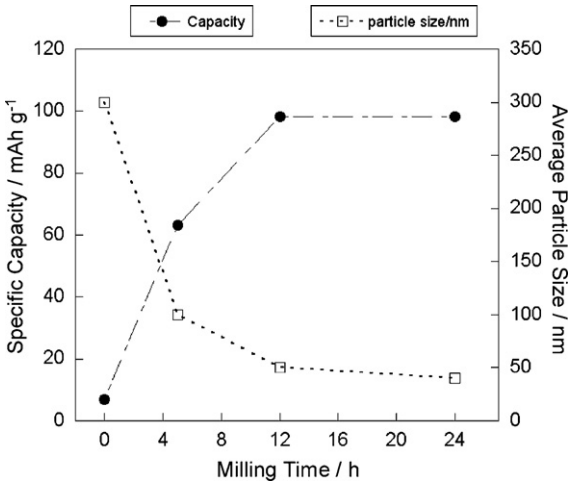

Fig. 9. Variation of reversible specific capacity (left *y*-axis) at 0.1 mA cm^{-2} and average particle size (right *y*-axis) with milling time.

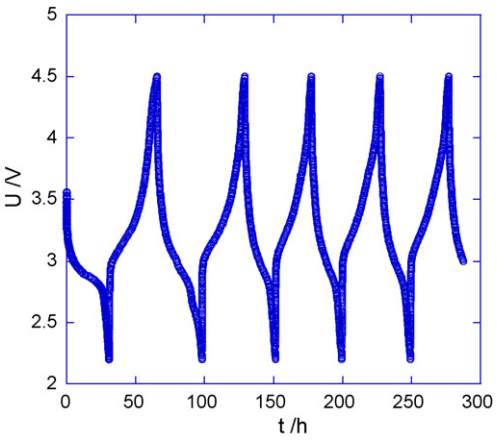

Fig. 10. Voltage *vs.* time plot of a Li/α-Li_3FeF_6 cell using a 12 h-milled composite as the positive electrode (current density: 0.1 mA cm^{-2}).

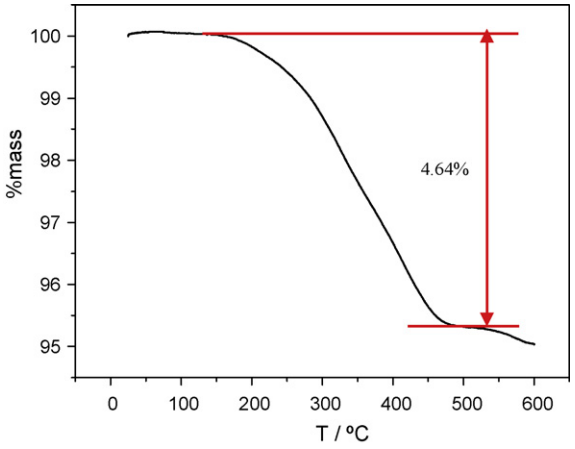

Fig. 11. TG curve for α-Li_3FeF_6 in nitrogen with traces of oxygen and water with a heating rate of 10 K min^{-1}.

Although further reduction of particle size as well as a more homogeneous distribution of sizes will be required for reaching the maximum capacity and optimized cycling behaviour our electrochemical results already point to α-Li_3FeF_6 as a very promising candidate to cathode for lithium batteries.

Another important characteristic of α-Li_3FeF_6 is its thermal stability over a quite broad temperature range and under ambient atmosphere. Fig. 11 shows the result of a TG experiment carried out under inert gas (nitrogen) containing small amounts of water and oxygen. No significant weight loss is detected up to 200 °C. Above 200 °C a steadily weight loss reaching 4.64% of its initial weight is attributed to partial hydrolysis accordingly to the reaction:

$$Li_3FeF_6 + (3/2)H_2O \rightarrow 3LiF + 3HF + (1/2)Fe_2O_3 \quad (2)$$

Weak reflections coming from LiF and Fe_2O_3, besides α-Li_3FeF_6, are detected in the XRD pattern after a heating cycle to 600 °C. LiF and Fe_2O_3 are the sole phases observed when α-Li_3FeF_6 is heated at 600 °C in air, indicating that complete hydrolysis is accomplished under these conditions. Interestingly, other fluorides including FeF_3, which has been recently proposed as electrode material, seems to be hygroscopic at room temperature since reported procedures include milling under helium and opening of the milling cell under an argon atmosphere [14,17]. However, we have found that monoclinic (α) Li_3FeF_6 is a non-hygroscopic substance that can be easily dried in air at 100 °C without decomposition. Thus, advantageously the handling of the electrode material α-Li_3FeF_6 can be made in air.

Therefore, if we take into consideration that monoclinic Li_3FeF_6:

(i) can be prepared at temperatures between 25 and 60 °C with already submicrometric particle size;
(ii) the electrochemical active transition metal is iron, an environment friendly element;
(iii) specific capacities of ca. 100 mA h g^{-1} can be easily achieved through an intercalation reaction likely involving the reduction of Fe^{3+} to Fe^{2+}; and
(iv) it does not suffer hydrolysis at ambient conditions.

we propose α-Li_3FeF_6 as a promising cathode [20] material that deserves attention to be optimized through proper processing to reach more reliable electrochemical performances. Presently, both output voltage and theoretical capacity are not high enough to rival $LiFePO_4$ performances but the facile preparation method of Li_3FeF_6 is an important advantage. However, more efforts need to be made to reach at least the theoretical capacity (140 mA h g^{-1}) which include the investigations of synthesis methods that provide nanosized particles to avoid the ball milling process.

4. Conclusions

We have synthesized monoclinic α-Li_3FeF_6, which adopts a distorted cryolite-type structure, for the first time using an aqueous solution-based route at moderate temperature (between 20 and 60 °C).

While the electrochemical performances of as-prepared Li_3FeF_6 are rather poor, capacity can be increased when the fluoride is dry ball milled in presence of carbon black. After 12 h milling time a reversible capacity of 100 mA h g^{-1} is displayed at ca. 3.1 V, which is 70% of the theoretical specific capacity expected for Fe^{3+} to Fe^{2+} in Li_3FeF_6 content (140 mA h g^{-1}). Although both output voltage and theoretical capacity are not high enough to rival $LiFePO_4$ performances, the facile preparation method of Li_3FeF_6 is an important advantage. Besides, taking into account its chemical and thermal stability, clearly above 100 °C, α-Li_3FeF_6, the monoclinic form of Li_3FeF_6, may be proposed as a new and very promising candidate to cathode applications in lithium batteries. However, more efforts need to be made to reach at least the theoretical capacity, which include the investigations of synthesis methods that provide nanosized particles to avoid the ball milling process.

Acknowledgments

The authors thank Ministerio de Ciencia e Innovación (MICINN) and Comunidad de Madrid (CAM) for funding the projects MAT2007-64486-C07-01 and S-0505/PPQ/0358, respectively. Financial support from Universidad CEU San Pablo is also acknowledged. E.G. thanks Universidad CEU San Pablo for a predoctoral grant.

References

[1] K. Mizushima, P.C. Jones, P.J. Wiseman, J.B. Goodenough, Materials Research Bulletin 15 (1980) 783–789.
[2] J.M. Tarascon, E. Wang, F.K. Shokoohi, W.R. McKinnon, S. Colson, Journal of the Electrochemical Society 138 (1991) 2859–2864.
[3] J.K. Kim, A. Manthiram, Nature 390 (1997) 265–267.
[4] A.K. Padhi, K.S. Nanjundaswamy, J.B. Goodenough, Journal of the Electrochemical Society 144 (1997) 1188–1194.
[5] Q.M. Zhong, A. Bonakdarpour, M.J. Zhang, Y. Gao, J.R. Dahn, Journal of the Electrochemical Society 144 (1997) 205–213.
[6] Y. Ein-Eli, W.F. Howard, S.H. Lu, S. Mukerjee, J. McBreen, J.T. Vaughey, M.M. Thackeray, Journal of the Electrochemical Society 145 (1998) 1238–1244.
[7] C. Masquelier, A.K. Padhi, K.S. Nanjundaswamy, J.B. Goodenough, Journal of Solid State Chemistry 135 (1998) 228–234.
[8] J.M. Paulsen, C.L. Thomas, J.R. Dahn, Journal of the Electrochemical Society 147 (2000) 861–868.
[9] P.G. Bruce, A.R. Armstrong, R.L. Gitzendanner, Journal of Materials Chemistry 9 (1999) 193–198.
[10] H. Kawai, M. Nagata, H. Tukamoto, A.R. West, Electrochemical and Solid State Letters 1 (1998) 212–214.
[11] R. Kanno, T. Shirane, Y. Kawamoto, Y. Takeda, M. Takano, M. Ohashi, Y. Yamaguchi, Journal of the Electrochemical Society 143 (1996) 2435–2442.
[12] J.M. Cocciantelli, J.P. Doumerc, M. Pouchard, M. Broussely, J. Labat, Journal of Power Sources 34 (1991) 103–111.
[13] C. Sigala, D. Guyomard, A. Verbaere, Y. Piffard, M. Tournoux, Solid State Ionics 81 (1995) 167–170.
[14] P.N. Badway, F. Cosandey, G.G. Amatucci, Journal of the Electrochemical Society 150 (2003) A1209–A1218.
[15] H. Arai, S. Okada, Y. Sakurai, J. Yamaki, Journal of Power Sources 68 (1997) 716–719.
[16] Y. Koyama, I. Tanaka, H. Adachi, Journal of the Electrochemical Society 147 (2000) 3633–3636.
[17] I.D. Gocheva, M. Nishijima, T. Doi, S. Okada, J. Yamaki, T. Nishida, Journal of Power Sources 187 (2009) 247–252.
[18] M. Nishijima, I.D. Gocheva, S. Okada, T. Doi, J. Yamaki, T. Nishida, Journal of Power Sources 190 (2009) 558–562.
[19] G.G. Amatucci, "Metal Fluorides as Electrode Materials". Patent US 7,371,338. 25 November 2003.
[20] F. García Alvarado, A. Kuhn, E. Gonzalo, "Electrodo Catódico Li–Fe–F para baterías recargables de litio y de ión litio, preparado a partir de disoluciones acuosas a temperatura ambiente." Patent Apl. no. P20091993 SPAIN. 14 October 2009.
[21] A.H. Nielsen, Zeitschrift fur Anorganische und Allgemeine Chemie 224 (1935) 84.

[22] A. Tressaud, J. Portier, S. Shearer-Turrell, J.-L. Dupin, P. Hagenmuller, Journal of Inorganic and Nuclear Chemistry 32 (1970) 2179–2186.
[23] W. Massa, W. Rüdorff, Zeitschrift fur Naturforsch 26b (1971) 1216–1218.
[24] J.L. Holm, B. Jenssen, Acta Chemica Scandinavica 23 (1969) 1065–1068.
[25] G. Garton, B.M. Wanklyn, Journal of Inorganic & Nuclear Chemistry 27 (1965) 2466–2469.
[26] A.K. Tyagi, J. Kohler, Materials Research Bulletin 32 (1997) 1683–1689.
[27] J.H. Burns, A.C. Tennisse, G.D. Brunton, Acta Crystallographica Section B-Structural Crystallography and Crystal Chemistry B 24 (1968) 225–230.
[28] A. Kuhn, E. Gonzalo, F. García Alvarado, To be published elsewhere (2010).
[29] E. Gonzalo, A. Kuhn, F. García-Alvarado, ECS Transactions 14 (2010) 9–18.
[30] H.M. Rietveld, Acta Crystallographica 22 (1967) 151–152.
[31] J. Rodriguez Carvajal, Physica B 192 (1993) 55–69.
[32] M. Gaberscek, R. Dominko, M. Bele, M. Remskar, D. Hanzel, J. Jamnik, Solid State Ionics 176 (2005) 1801–1805.
[33] K.F. Hsu, S.Y. Tsay, B.J. Hwang, Journal of Materials Chemistry 14 (2004) 2690–2695.
[34] R. Dominko, M. Bele, M. Gaberscek, M. Remskar, D. Hanzel, S. Pejovnik, J. Jamnik, Journal of the Electrochemical Society 152 (2005) A607–A610.
[35] Y.Q. Hu, M.M. Doeff, R. Kostecki, R. Finones, Journal of the Electrochemical Society 151 (2004) A1279–A1285.
[36] M.M. Doeff, Y.Q. Hu, F. McLarnon, R. Kostecki, Electrochemical and Solid State Letters 6 (2003) A207–A209.
[37] Z.H. Chen, J.R. Dahn, Journal of the Electrochemical Society 149 (2002) A1184–A1189.